STScI | SPACE TELESCOPE SCIENCE INSTITUTE

**Instrument Science Report ACS ISR 2019-08**

# Temporal Stability of the ACS/WFC OD-800W LED.

N. D. Miles & N. A. Grogin

September 16, 2019

Abstract

*This report summarizes an analysis of the ACS/WFC post-flash LED stability over a ∼4.5 year period. We analyze 1,294 post-flash calibration darks generated from January 2015 to July 2019. We find the observed intensity of the LED, relative to the intensity in January of 2015, to be declining at a rate of ∼ 0.2% per year. We use the resulting fit to the LED signal over time to compute a time-dependent normalization factor for each annual post-flash reference file. This normalization reduces the observed scatter between the post-flash reference files caused by short-term fluctuations in the intensity of the LED. The normalized post-flash reference files are currently available in the HST Calibration Reference Data System (CRDS)*[1].

## 1 Introduction

Over the course of its ∼18 year lifetime, the Opto Diode OD-800W LED attached to the ACS/WFC instrument housing has been continuously irradiated by space weather, particles trapped in the Van Allen radiation belts, and galactic cosmic rays. The OD-800W LED was designed to have a fast response, a high power output, excellent power degradation characteristics, and a high radiation tolerance (Opto Diode 2017). It is used to artificially raise the background level in ACS/WFC images to alleviate the effects of an imperfect charge transfer efficiency (CTE), but has limited applicability due to the noise imparted by the post-flash correction. Throughout the operational lifetime of the ACS/WFC, the LED has been used to post-flash a total of 5,688 observations for a cumulative flash duration of 18.4 hours (see Figure 1).

[1] https://hst-crds.stsci.edu

The cumulative usage of the ACS/WFC OD-800W LED represents a very small fraction of its expected lifetime. Lab testing by Opto Diode demonstrated that the LED could be continuously operated for more than 10,000 hours before observing any losses in the LED power output (Opto Diode 2017). In 2015, the ACS Team began routinely using the LED to generate post-flash calibration darks. This change resulted in an on/off cycling of the LED at a rate of 18 times per week. The manufacturer reported that no lab tests were performed to assess the effect of on/off cycling rates on the total lifetime of the OD-800W LED. However, they stated that consistently cycling the LED on/off could potentially mitigate the degradation as it reduces the amount of self-heating the LED is exposed to (priv. communication, Opto Diode). For completeness, we note that some studies have shown that a constant on/off cycling can decrease the lifetime of an LED, but they typically analyze generic commercial LEDs which likely exhibit vastly different lifetime characteristics than a radiation hardened LED like the OD-800W (see e.g. Narendran et al. 2015).

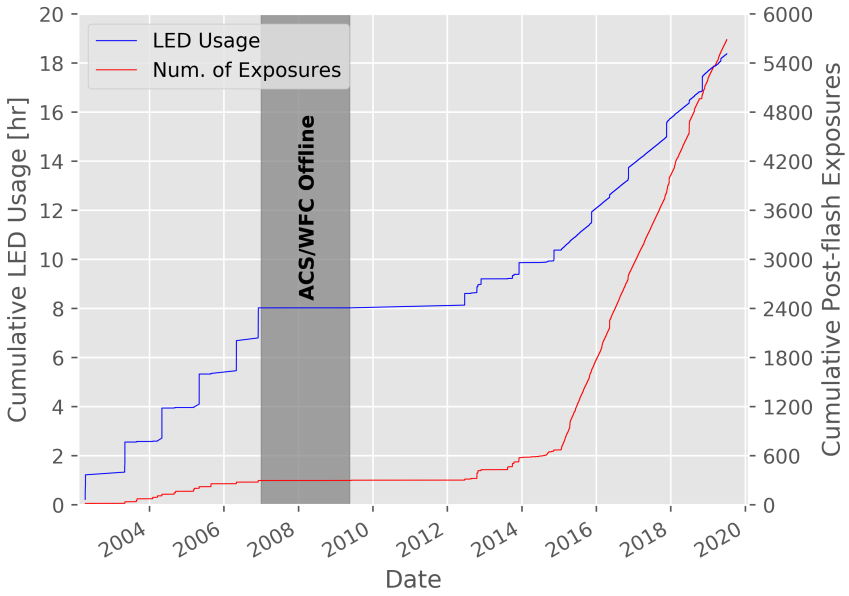


**Figure 1:** The lifetime usage of the ACS/WFC Opto Diode OD-800W LED. On the left-most y axis, we show the cumulative LED usage in hours over the lifetime of the instrument denoted by the blue line. On the right-most y axis, we show the cumulative number of post-flashed exposures over the lifetime of the instrument denoted by the red line.

In the following sections we describe our stability analysis of the ACS/WFC LED. In Section 2, we review the key findings from previous studies of the ACS/WFC LED behavior. In Section 3, we motivate our work by reproducing the analysis of Miles (2018) using additional observations taken as part of the most recent post-flash calibration program. In Section 4, we describe the dataset used to probe the temporal stability of the LED. In Section 5, we detail the methods used to measure the LED signal. In Sections 6 and 7, we describe the modeling of dark current and cosmic rays contributions, respectively. In Section 8, we analyze the LED signal as a function of time. Lastly, in Section 9 we detail the normalization process applied to reduce the scatter in our post-flash reference files.

# 2 Previous Studies

Cox (2006) performed the initial evaluation and characterization of the ACS/WFC post-flash LED and found that from 2003 to 2006 the post-flash LED remained stable. Ogaz et al. (2014) evaluated the post-flash capabilities as a means to ameliorate the effects of imperfect CTE. They examined the temporal stability and confirmed the original findings of Cox (2006), but noted a significant decrease in the overall signal from 2006 to 2012; in a 400 second shutter A exposure, the high and medium intensity signal dropped by approximately 30%, and the low intensity signal by approximately 20%. Bellini et al. (2017) probed the temporal stability of the post-flash LED while evaluating post-flash subarray modes. Ultimately, they found that the intensity of the LED had remained stable between November 2015 and May 2016. Lastly, Miles (2018) assessed the temporal stability of the LED by analyzing all post-flash reference files generated since 2012. They found that although there was an apparent decline in LED intensity at a rate of $\sim$0.3% per year from 2013 to 2016, the full dataset from 2012 to 2017 was statistically consistent (at the $1\sigma$ level) with a constant value.

# 3 Motivation

Observations from the second iteration of the updated post-flash calibration program (proposal ID: 15531) were obtained in November of 2018. Prior to Cycle 25, the post-flash calibration program took a series of long flash exposure that were then bias corrected, dark subtracted, and combined to reject cosmic rays to produce the post-flash calibration reference file. In Cycle 25, the post-flash calibration program was updated to begin taking two groups of observations with a fixed DARKTIME ($t_D$). DARKTIME is given by the sum of the commanded exposure time ($t_E$), the commanded flash duration ($t_F$), and any overheads ($\delta t$) associated with commanding. The first group of observations has an EXPTIME of 0.5s and a FLASHDUR of 341.0s, whereas the second the group has an EXPTIME of 337.0s and a FLASHDUR of 4.5s. Since the commanding overheads are consistent from image to image we have $t_{D1} = t_{D2}$. Each group of observations is bias corrected and then combined to reject cosmic rays. Using the combined long-flash observation ($p_1$) and the combined short-flash observation ($p_2$), we subtract off the dark current and isolate the LED signal as follows:

$$\begin{aligned} p_{final}(x,y) =& p_1(x,y) - p_2(x,y) \\ =& [t_{D1} * dc(x,y) + t_{F1} * fr(x,y)] \\ & - [t_{D2} * dc(x,y) + t_{F2} * fr(x,y)] \\ =& (t_{F1} - t_{F2}) * fr(x,y) \\ fr(x,y) =& \frac{p_{final}(x,y)}{t_{F1} - t_{F2}} \end{aligned} \tag{1}$$

After generating the post-flash reference file for 2018 using the methodology listed above, the boxed mean analysis from Section 4.2 of Miles (2018) was repeated to include the additional datum. 27 samplings of LED intensity were measured around the detector using 100x50-pixel boxes to determine mean pixel value and mean standard deviation. The mean

pixel value is computed as the mean of the box in the SCI extension. The mean standard deviation, $\langle\sigma\rangle$, is computed as the mean of the box applied to the ERR extension. This is done to avoid confusing spatial variations in the LED illumination pattern with the per pixel error. In Figure 2, we show the results for two boxes, zoomed in to highlight the fluctuations over time.

Overall, we found that the post-flash reference file in 2018 shows a ∼3% drop in the mean value of each box, when compared to the post-flash reference file from 2017. While the error bars denote the average per pixel uncertainty for pixels in the 100 pixel by 50 pixel box, the true error on the boxed mean measurement (i.e. the standard deviation of the mean) is given by $\langle\sigma\rangle/\sqrt{100 * 50}$. This yields an error of $\sim$ 0.00025 electrons per second. The only measurements agreeing within a $5\langle\sigma\rangle$ level are late 2015 and late 2016, and with the addition of the 2018 datum the LED intensity appears to be declining over time.

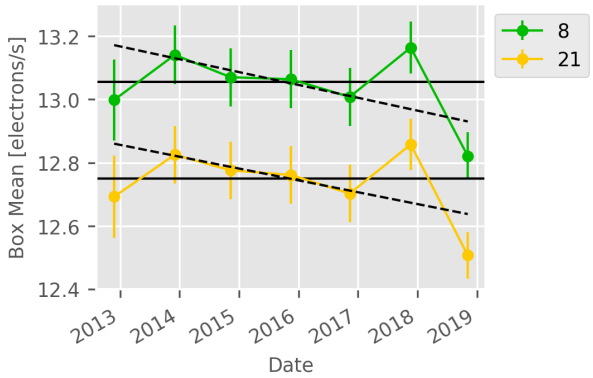


**Figure 2:** The means for box 8 and 21 computed using the post-flash reference files from late 2012 to late 2018. The errorbars denote per-pixel uncertainty. The dashed lines are linear fits to the 2013-2016 post-flash reference files only. The horizontal solid lines denote the mean of each set of datapoints.

# 4 Dataset

To probe the temporal stability of the ACS/WFC LED, we analyze all short exposure, post-flashed dark frames taken as part of the routine CCD Daily Monitor calibration programs. The ACS Team began generating post-flash calibration darks (Ogaz et al. 2015) partway through Cycle 22 in 2015 and so the our dataset spans from January 2015 to present day. Each short dark has an EXPTIME of 0.5s and a FLASHDUR of 4.6s. We processed each file through CALACS (v. 10.1.0) with DQICORR, BIASCORR, BLEVCORR, and SINKCORR set to PERFORM and everything else to OMIT. The end result is 1,294 post-flashed, short darks that have had sink pixels flagged (Ryon et al. 2017a) and the contributions from the bias and readout dark removed (Ryon et al. 2017b).

After processing, each image will have units of electrons. For each pixel, the remaining signal is a linear combination of the LED signal, any accumulated dark current, and any electrons deposited by cosmic rays. If we let $fr(x, y)$ represent the LED count rate in electrons per second, $dc(x, y)$ represent the dark current in electrons per second, and $cr(x, y)$ represent the electron deposition per second by cosmic rays, then the final pixel value is

given by:

$$p(x,y) = t_F * fr(x,y) + t_D * dc(x,y) + t_C * cr(x,y) \tag{2}$$

Where $t_F$ is the commanded flash duration denoted by the FLASHDUR keyword; $t_D$ is the total time over which dark current accumulated and is given by the DARKTIME keyword (Lucas et al. 2018); $t_C$ is the total time over which cosmic rays impacts are recorded by the detector and is defined as the sum of the DARKTIME and half the readout time (∼50s). Half of the readout time is added to account for cosmic ray strikes that occur during the readout process, while the original image is being shifted off the CCDs and into the serial registers for readout.

# 5 Methodology

To monitor the power output of the LED as a function of time, we compute the average value per pixel for each short dark using the entire detector which is 4096 pixels by 4096 pixels:

$$\langle p \rangle = \frac{1}{4096 * 4096} \sum_{x=1}^{4096} \sum_{y=1}^{4096} p(x,y) \tag{3}$$

Substituting Equation 2 for $p(x,y)$, we find that the average signal in electrons per pixel is given by

$$\langle p \rangle = \frac{1}{4096 * 4096} \sum_{x=1}^{4096} \sum_{y=1}^{4096} [t_F * fr(x,y) + t_D * dc(x,y) + t_C * cr(x,y)] \tag{4}$$

$$= t_F * \langle fr \rangle + t_D * \langle dc \rangle + t_C * \langle cr \rangle \tag{5}$$

Solving for the average flash rate, $\langle fr \rangle$, we find,

$$\langle fr \rangle = \frac{\langle p \rangle - t_D * \langle dc \rangle - t_C * \langle cr \rangle}{t_F} \tag{6}$$

Finally, from Figure 2, it is safe to assume that the average value per pixel in the short darks, $\langle p \rangle$, is decreasing with time. Next, it has long been known that the average dark rate, $\langle dc \rangle$, of the ACS/WFC CCD's has been steadily increasing over the lifetime of ACS (Ubeda et al. 2012, Ryon et al. 2019). Lastly, the observed cosmic ray flux is also changing with time due to changes in solar activity (Hathaway 2015). Hence, the final expression for the average flash rate at time, $t$, is given by,

$$\langle fr \rangle(t) = \frac{\langle p \rangle(t) - t_D * \langle dc \rangle(t) - t_C * \langle cr \rangle(t)}{t_F} \tag{7}$$

# 6 Modeling Dark Current

To estimate the dark current present in each image, we fit a linear model to the average dark rate as a function of time. Using the ACS/WFC superdarks, we compute the average dark rate per pixel as

$$\langle dc \rangle = \frac{1}{4096 * 4096} \sum_{x=1}^{4096} \sum_{y=1}^{4096} dc(x,y). \tag{8}$$

We use the python package `pymc3` (Salvatier et al. 2016) to perform Bayesian linear regression and determine the rate of increase of the average dark rate as a function of time. We assume Gaussian distributed priors for the slope ($m$) and intercept ($b$). The most probable values, their $1\sigma$ errors, and their 95% highest posterior density intervals are listed in Table 1. The resulting fit is plotted with the data in Figure 3.

**Table 1:** Fit results for the average dark rate as function of time, $\langle dc \rangle(t)$.

| | Most Probable | Error | 95% Highest Posterior Density |
|---|---|---|---|
| $b$ [$e^-$/s] | -0.180 | 0.005 | (-0.189, -0.170) |
| $m$ [$e^-$/s/pixel/day] | $3.63 \times 10^{-6}$ | $8.72 \times 10^{-8}$ | ($3.46 \times 10^{-6}$, $3.79 \times 10^{-6}$) |

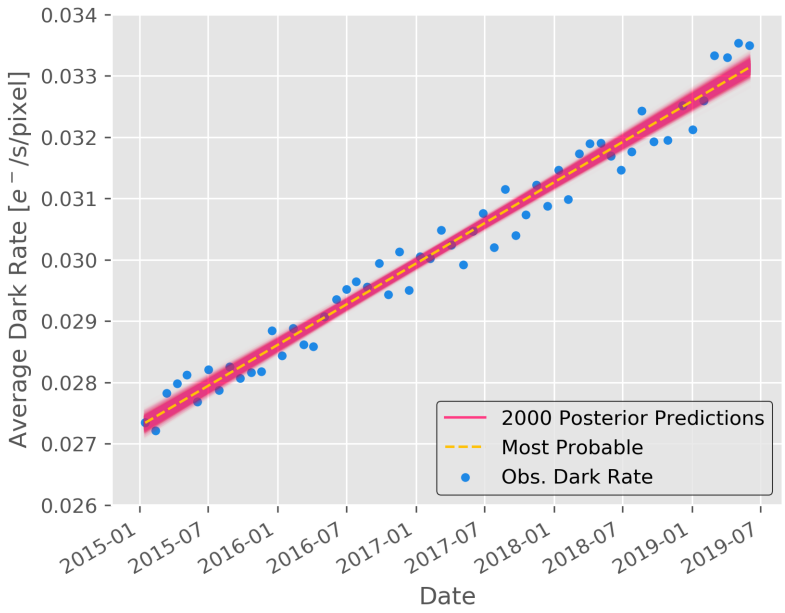


**Figure 3:** The average dark rate computed from the ACS/WFC superdarks. Error bars are smaller than the markers. The dashed, yellow line represents the most probable (i.e. best-fit) solution from the posterior distribution. The solid, gray lines represent 2000 random draws from the posterior distribution.

# 7 Modeling Cosmic Rays

To model the behavior of cosmic rays, we utilize the same connected-component labeling algorithm detailed in Appendix A of Miles (2018). We analyze 3,860 dark calibration frames spanning the same time period of the short darks dataset (2015 to 2019). For each image, we compute the cumulative number of electrons per pixel per second deposited by cosmic rays across the entire detector as,

$$\langle cr \rangle = \frac{1}{4096 * 4096} \sum_{x=1}^{4096} \sum_{y=1}^{4096} cr(x, y) \tag{9}$$

where $cr(x, y)$ is the value of the pixel at $(x, y)$ if it was affected by a cosmic ray during the observations and 0 otherwise. A pixel is determined to be affected by a cosmic ray if it is

marked in the DQ array during the cosmic ray rejection step, ASCREJ, of CALACS.

The observed cosmic ray flux varies over long baselines due to changes in solar activity as the Sun progresses through its 11 year solar cycle. Our short dark dataset samples the last half of Solar Cycle 24 which began in 2008 and is predicted to end at the end of 2019. Due to the uncharacteristically weak nature of Solar Cycle 24 (Basu 2013), we expect to see little variation in the baseline cosmic ray flux over the 4 year period. In Figure 4, we show the distribution of the cumulative number of electrons deposited per pixel per second by cosmic rays in each of the 3,860 dark calibration frames analyzed.

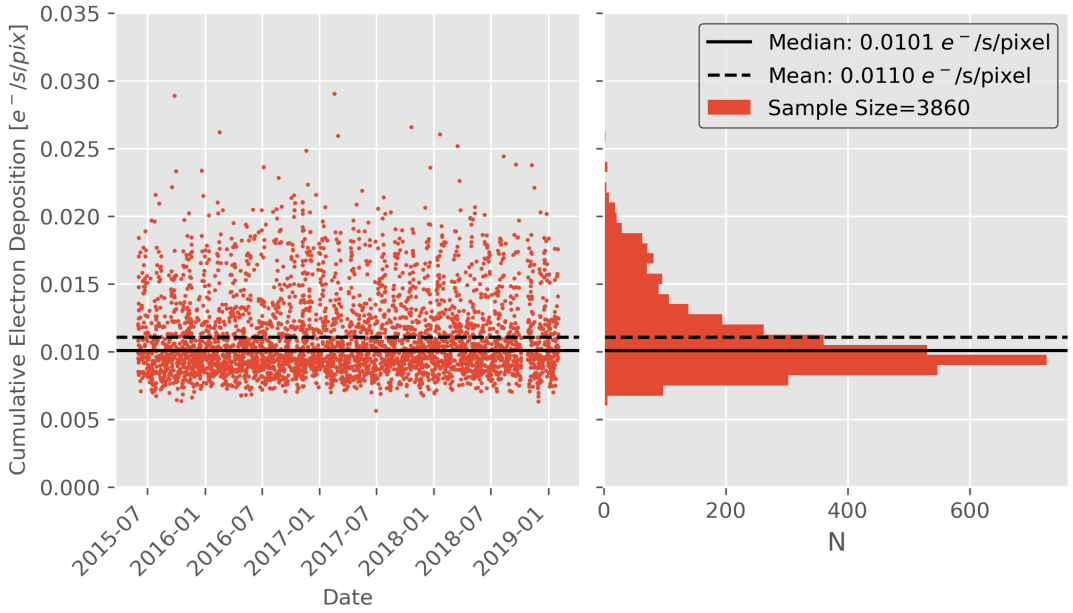


**Figure 4:** The distribution of the total number of electrons deposited per second per pixel by cosmic rays.

The average cumulative energy deposited by cosmic rays from January 2015 to January 2019 is 0.011 $\pm$ 0.0031 $e^-$/s/pixel. The average cumulative energy deposited by cosmic rays remains fairly stable over the time period with 84% of the measurements falling within one standard deviation of the mean, while the instantaneous value fluctuates on timescales much shorter than the solar cycle. The driver of the short timescale fluctuations in currently unknown. Because of this we use the mean cumulative energy deposited per second per pixel, 0.011$e^-$/s/pixel as a representative value for modeling contributions from cosmic rays at any time, $t$, over the 4 year period.

# 8 Analyzing the LED Signal

With models characterizing the contributions from the dark current and cosmic rays, we can now compute the average flash rate in electrons per second per pixel. Substituting the models into Equation 10 yields,

$$\langle fr \rangle(t) = \frac{\langle p \rangle(t) - t_D * (3.63 \times 10^{-6} * t - 0.18) - t_C * (0.011)}{t_F} \tag{10}$$

We validate our modeling by comparing the average flash rate derived from the short darks to the average flash rate derived from the post-flash calibration reference files. They are created from long duration post-flash exposures that have been bias and dark corrected, as well as, stacked together to produce a final cosmic ray cleaned image with no dark current or cosmic ray contributions. In Figure 5, we plot the average flash rates derived from the un-modeled data, the modeled data, and the post-flash reference files. After modeling contributions from dark current and cosmic rays, we find the average flash rate from the short darks and the post-flash reference files to be in agreement with one another.

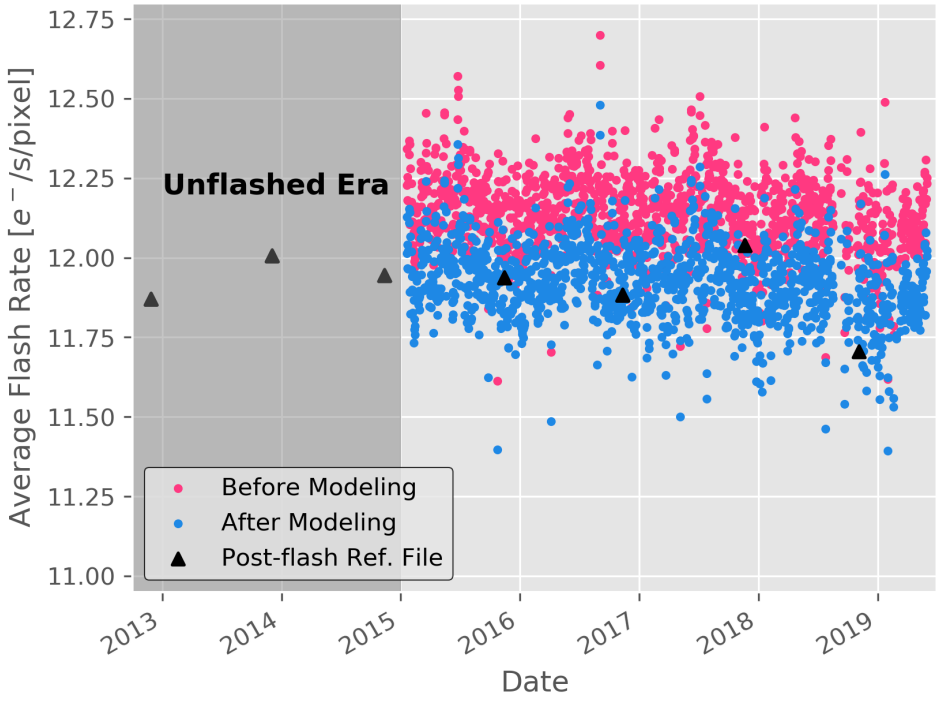


**Figure 5:** The average flash rate computed before and after modeling contributions from the dark current and cosmic rays.

To derive the rate of decline in the LED power output, we repeat the Bayesian analysis performed in Section 6 using the average flash rate after modeling contributions from dark current and cosmic rays. We again assume Gaussian distributed priors for the slope ($m$) and intercept ($b$). The most probable values, their $1\sigma$ errors, and their 95% highest posterior density intervals are listed in Table 2. The resulting fit is plotted with the data in Figure 6.

**Table 2:** Fit results for the average flash rate as function of time, $\langle fr \rangle(t)$.

| | Most Probable | Error | 95% Highest Posterior Density |
|---|---|---|---|
| $b$ [$e^-$/s] | 15.71 | 0.41 | (14.97, 16.53) |
| $m$ [$e^-$/s/pixel/day] | $-6.62 \times 10^{-5}$ | $7.03 \times 10^{-7}$ | $(-7.97 \times 10^{-5}$ , $-5.27 \times 10^{-5})$ |

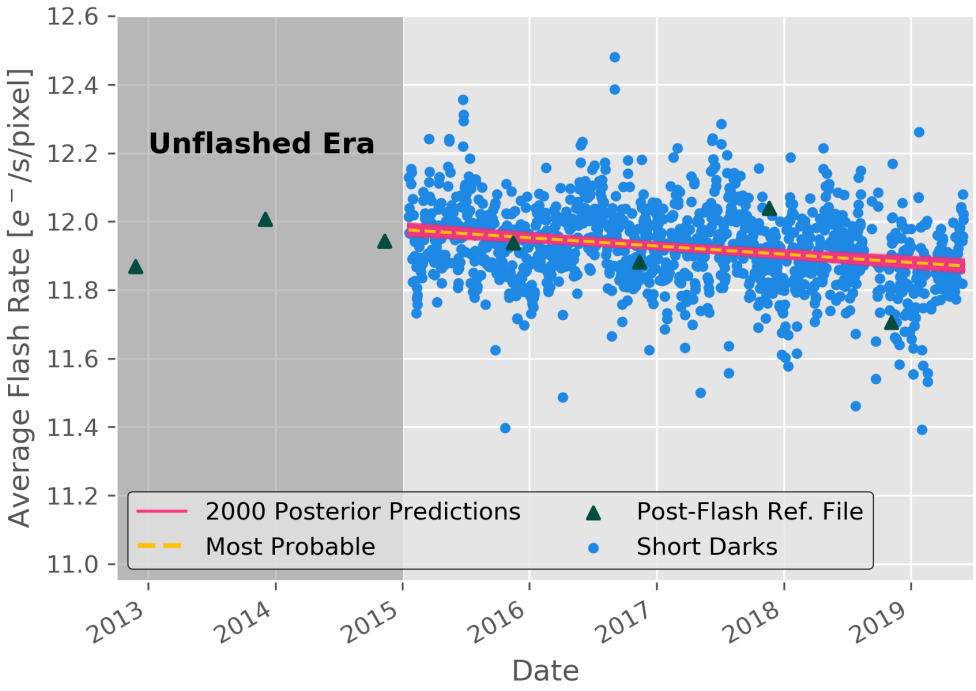


**Figure 6:** The average flash rate computed from the short darks. The dashed, yellow line represents the most probable (i.e. best-fit) solution from the posterior distribution. The solid, gray lines represent 2000 random draws from the posterior distribution. Note that the error bar for each measurement is smaller than the marker.

We compute the average percent loss in the LED flash rate starting from 2015 and find that the power output is decreasing at a rate of $\sim 0.2\%$ per year. Note, however, that this value represents the combined loss of the CCD sensitivity and the LED's power output. In the most recent analysis of the ACS sensitivity, Bohlin (2016) found an average sensitivity loss of 0.06%. Hence, the actual decline in the LED power output may be as low as 0.14%. In Figure 7, we compare the rate of decline of the LED power output and the rate of increase of the average dark rate. Over the four year period from 2015-2019, the LED power output dropped by $\sim 0.8\%$ while the average dark rate increased by $\sim 20\%$. Even though the contribution from the dark current in a DARKTIME of $\sim 11.25$ seconds is fractionally small, the accelerated growth rate of the dark current over time is enough to flatten the observed rate of decrease in the power output LED by 14.04% to $5.69 \times 10^{-5}$ $e^-$/s/pixel/day.

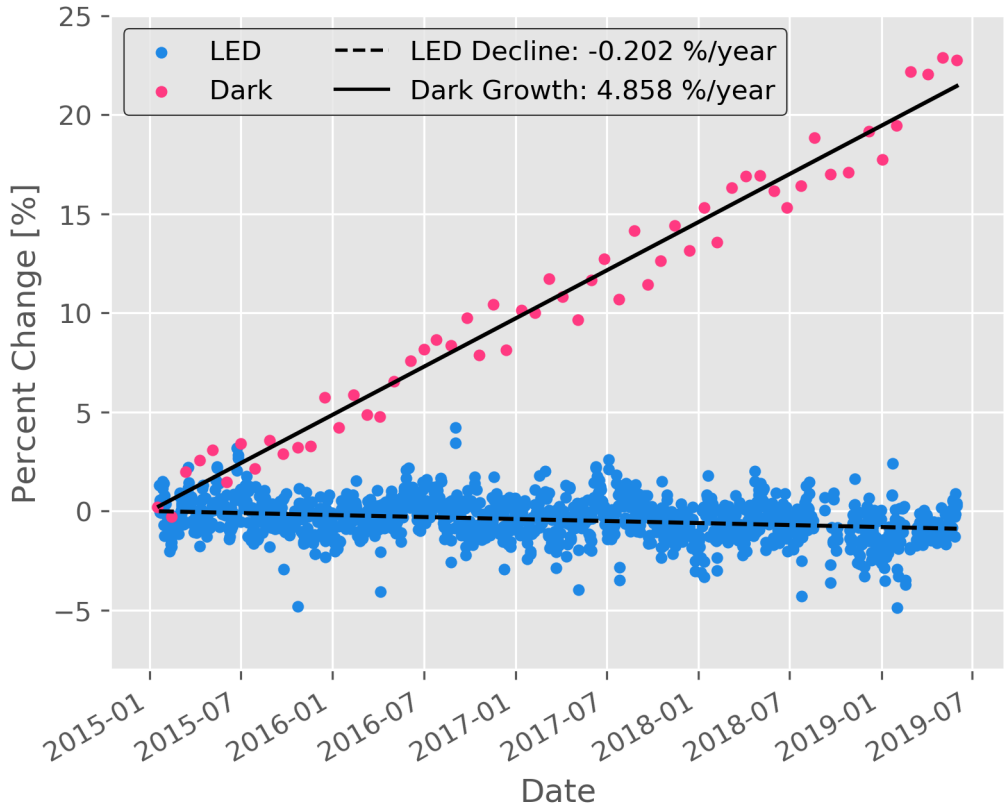


**Figure 7:** A comparison of the rate of change of average dark rate and the average flash rate. Error bars are smaller than the markers. For both datasets, we define January 1st, 2015 to be the starting point and compute the percent change over time from that date.

# 9 Normalizing Post-flash Reference Files

In Figure 6, we see that the scatter in the average flash rate computed using the post-flash reference files is within the scatter of the average flash rate computed using the short darks. The origin of the scatter in the average flash rate is currently thought to be driven by temperature fluctuations in local environment of the LED (see Miles 2018). At the present moment the infrastructure required for implementing a temperature-dependent post-flash correction does not exist. However, the ACS Team plans to investigate the feasibility of establishing the necessary infrastructure to accommodate a temperature-dependent post-flash correction.

So, while we may not be able to remove the scatter caused by temperature fluctuations, we can reduce the observed scatter in the post-flash reference files by normalizing them to their value predicted by the linear fits in Section 8. Using the fit information from Table 2, we compute a time-dependent scaling factor ($\alpha(t)$) for each post-flash reference file. We define $\alpha(t)$ as,

$$\alpha(t) = \frac{-6.62 \times 10^{-5} * t + 15.71}{\langle fr \rangle (t)} \tag{11}$$

where $t$ is the average MJD date of the set of observations used to create the post-flash reference file and $\langle fr \rangle(t)$ is the average flash rate of the post-flash reference file. The scaling factor is then applied as a multiplicative factor to normalize each `SCI` and `ERR` extension of the post-flash reference files. After applying the scaling factors, the post-flash reference files more closely represent the average power output of the LED with respect to it's nominal operating termperature. In Figure 8, we show the results of the normalization.

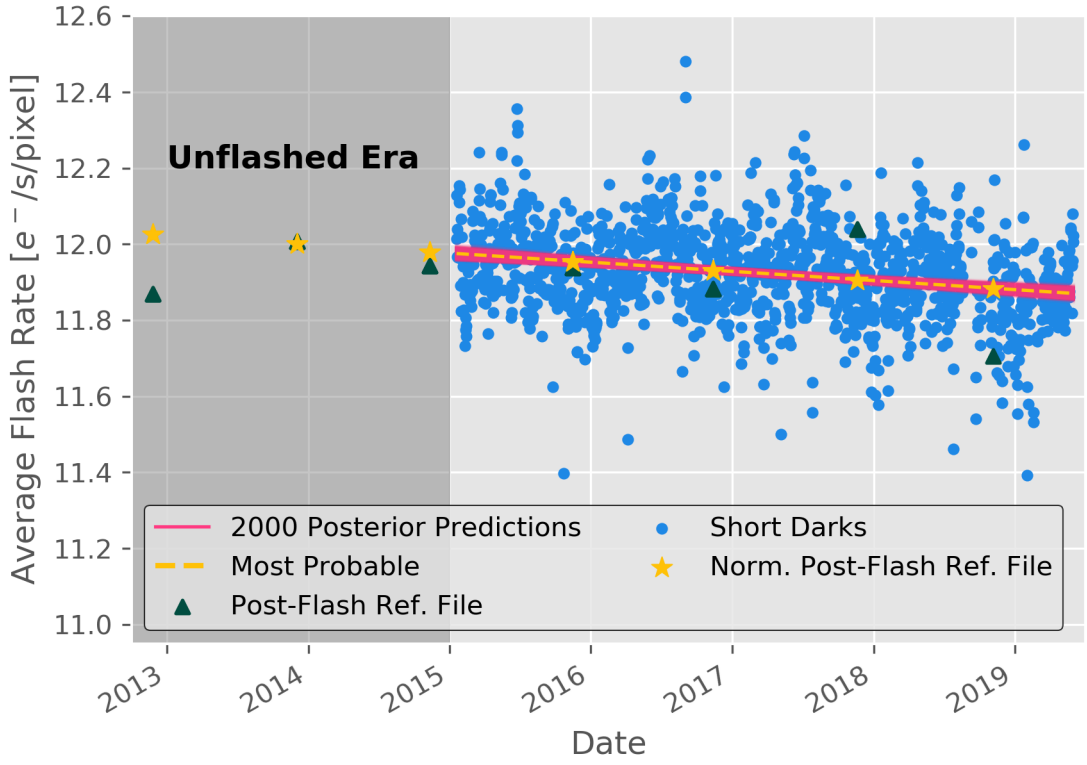


**Figure 8:** A comparison of the average flash rate derived from the post-flash reference files before and after the normalization process.

# 10 Conclusion

Overall we find that the ACS/WFC LED is operating nominally and the cumulative usage is well within the expected lifetime usage limits. By analyzing the post-flash short darks, we found that the LED intensity is slowly declining at a rate of $6.62 \times 10^{-5}$ $e^-$/s/pixel/day or $\sim 0.2\%$ per year since 2015. Using the fit results, we computed time-dependent scaling factors to renormalize each post-flash reference file to the trend line. The normalization process removes the intrinsic scatter caused by short-term fluctuations in the LED signal. The normalized post-flash reference files have been successfully ingested into CRDS and are currently available for use in the post-flash calibration step of `CALACS`.

# 11 Acknowledgements

The authors would like to thank the following ACS Team members, in no particular order, for their suggestions and feedback on this ISR: Jenna Ryon, Marco Chiaberge, Yotam Cohen, Ralph Bohlin, Samantha Hoffmann, and Nimish Hathi. This work made use of the following open source python packages: `astropy` (The Astropy Collaboration et al. 2018), `matplotlib` (Hunter 2007), `dask` (Dask Development Team 2016), `pandas` (McKinney 2010), `pymc3` (Salvatier et al. 2016), and `numpy` (van der Walt et al. 2011). Lastly, this work made use of the online colorblindness simulator, https://davidmathlogic.com/colorblind/, to derive a colorblind friendly palette suitable for protanopia, deuteranopia, and tritanopia.

# References

Basu, Sarbani (2013). "The peculiar solar cycle 24 – where do we stand?" In: *Journal of Physics: Conference Series* 440, p. 012001. DOI: 10.1088/1742-6596/440/1/012001. URL: https://doi.org/10.1088%2F1742-6596%2F440%2F1%2F012001.

Bellini, A., N.A. Grogin, P. L. Lim, and D. Golimowski (2017). *Post-Flash Validation of the new ACS/WFC Subarrays*. ACS ISR 2017-06. Space Telescope Science Institute.

Bohlin, Ralph C. (2016). "PERFECTING THE PHOTOMETRIC CALIBRATION OF THE ACS CCD CAMERAS". In: *The Astronomical Journal* 152.3, p. 60. DOI: 10.3847/0004-6256/152/3/60. URL: https://doi.org/10.3847%2F0004-6256%2F152%2F3%2F60.

Cox, C. (2006). *ACS Post-Flash Measurements*. ACS ISR 2006-07. Space Telescope Science Institute.

Dask Development Team (2016). *Dask: Library for dynamic task scheduling*. URL: https://dask.org.

Hathaway, David H. (2015). "The Solar Cycle". In: *Living Reviews in Solar Physics* 12.1, p. 4. ISSN: 1614-4961. DOI: 10.1007/lrsp-2015-4. URL: https://doi.org/10.1007/lrsp-2015-4.

Hunter, J. D. (2007). "Matplotlib: A 2D graphics environment". In: *Computing In Science & Engineering* 9.3, pp. 90–95. DOI: 10.1109/MCSE.2007.55. URL: https://matplotlib.org/devdocs/index.html.

Lucas, R.A. et al. (2018). *ACS Data Handbook*. Vol. 9.0. Space Telescope Science Institute.

McKinney, Wes (2010). "Data Structures for Statistical Computing in Python". In: *Proceedings of the 9th Python in Science Conference*. Ed. by Stéfan van der Walt and Jarrod Millman, pp. 51–56.

Miles, N.D. (2018). *Updates to Post-Flash Calibration for the Advanced Camera for Surveys Wide Field Channel*. ACS ISR 2018-03. Space Telescope Science Institute.

Narendran, Nadarajah and Yi-wei Liu (2015). "62.2: Invited Paper: LED Life Versus LED System Life". In: *SID Symposium Digest of Technical Papers* 46.1, pp. 919–922. DOI: 10.1002/sdtp.10402. eprint: https://onlinelibrary.wiley.com/doi/pdf/10.1002/sdtp.10402. URL: https://onlinelibrary.wiley.com/doi/abs/10.1002/sdtp.10402.

Ogaz, S., J. Anderson, and D. Golimowski (2015). *Post-Flash Calibration Darks for the Advanced Camera for Surveys Wide Field Channel (ACS/WFC)*. ACS ISR 2015-03. Space Telescope Science Institute.

Ogaz, S., M. Chiaberge, and N.A. Grogin (2014). *Post-Flash Capabilities of the Advanced Camera for Surveys Wide Field Channel*. ACS ISR 2014-01. Space Telescope Science Institute.

Opto Diode (2017). *OD800W Data Sheet*. URL: https://optodiode.com/pdf/OD800WDS.pdf (visited on 2017).

Ryon, J. E. and N. Grogin (2017a). *Sink Pixels in ACS/WFC*. Tech. rep.

Ryon, J. E., N. A. Grogin, and D. Coe (2017b). *Accounting for Readout Dark in ACS/WFC Superbiases*. ACS ISR 2017-13. Space Telescope Science Institute.

Ryon, J. E. et al. (2019). *Advanced Camera for Surveys Instrument Handbook*. Version 18. Space Telescope Science Institute, Baltimore MD.

Salvatier, John, Thomas V. Wiecki, and Christopher Fonnesbeck (2016). "Probabilistic programming in Python using PyMC3". In: *PeerJ Computer Science* 2, e55. ISSN: 2376-5992. DOI: 10.7717/peerj-cs.55. URL: https://doi.org/10.7717/peerj-cs.55.

The Astropy Collaboration et al. (2018). "The Astropy Project: Building an inclusive, open-science project and status of the v2.0 core package". In: *ArXiv e-prints*. arXiv: 1801.02634 [astro-ph.IM].

Ubeda, Leonardo and Jay Anderson (2012). *Study of the evolution of the ACS/WFC charge transfer efficiency*. ACS ISR 2012-03. Space Telescope Science Institute.

van der Walt, S., S. C. Colbert, and G. Varoquaux (2011). "The NumPy Array: A Structure for Efficient Numerical Computation". In: *Computing in Science Engineering* 13.2, pp. 22–30. ISSN: 1521-9615. DOI: 10.1109/MCSE.2011.37.